

# L1 Electrical conductivity degradation of fatigued carbon black L2 reinforced natural rubber composites: Effects of carbon L3 nanotubes and strain amplitudes

L4 E. Harea\*, S. Datta, M. Stěnička, R. Stoček

L5 Centre of Polymer Systems, Tomas Bata University in Zlín, Třída Tomáše Bati 5678, 760 01 Zlín, Czech Republic

L6 Received 13 May 2019; accepted in revised form 8 July 2019

L7 **Abstract.** The fatigue of rubber products is usually accompanied by undesirable transformation in their properties. The pres-  
 L8 ent work was dedicated to the investigation of consequences of fatigue loading on volume electric conductivity of natural  
 L9 rubber (NR) reinforced with 30 phr of fillers composed from various weight combinations of carbon nanotubes (CNTs) and  
 L10 carbon black (CB). Special attention was paid to study the influence of CNTs content on residual electric conductivity and  
 L11 a possible mechanism of fatigue driven rearrangement of hybrid filler network inside of rubber matrix was propounded for-  
 L12 ward. An increase in the CNTs content over the complete range of concentrations, enhanced the conductivity of fabricated  
 L13 samples up to two orders of magnitude in comparison to rubber compounds without CNTs. All the samples were subjected  
 L14 to harmonic sinusoidal loading at a frequency of 5 Hz up to  $10^5$  loading cycles at three different strains of 0.1, 0.25 and 0.5.  
 L15 Despite very little transformation in the polymer matrix, fatigue caused a progressive degradation of conductivity with an  
 L16 increase in applied strain. It was also found that with the addition and a subsequent increase in the concentration of CNTs,  
 L17 the undesirable reduction of conductivity was significantly arrested. This novel finding added another number to the list of  
 L18 the outstanding properties of CNTs.

L19 **Keywords:** rubber, fatigue, carbon nanotubes, electrical properties, hybrid fillers

## L20 1. Introduction

L21 Electrical conductivity of rubber compounds gained  
 L22 great interest since the fifties of the last century orig-  
 L23 inating from practical applications for antistatic tires,  
 L24 belts, electric cables and from fundamental relation-  
 L25 ship between conductivity and filler dispersion and  
 L26 reinforcement [1]. Nowadays, conductive elastomers  
 L27 are intensively studied as promising materials for  
 L28 transducers, sensors and flexible electrodes [2–5] be-  
 L29 cause of their ability to be elastically deformed while  
 L30 still providing some degree of electrical conductivity  
 L31 [6]. Usually, the aiming grade of conductivity is re-  
 L32 alized by filling an insulating polymer matrix with  
 L33 conductive particles [7]. Among the traditionally used  
 L34 types of fillers, fast development is in the direction

of using so called hybrid fillers which often exhibit  
 a synergetic effect in the properties of the composites  
 [8]. Suggestive examples are products from natural  
 rubber based composites filled with carbon nan-  
 otubes and carbon black hybrid fillers encompassing  
 noticeable enhancements in mechanical properties  
 such as fracture and fatigue resistance [9], friction  
 and wear [10], electrical properties [2, 11, 12] etc.  
 Higher conductivity of such a composite at lower  
 percolation threshold is achieved due to CB particles  
 which effectively bridge CNTs surrounded by non-  
 conductive polymer, and contributes to the formation  
 of new electron pathways.  
 During the service life, flexible electrodes, sensors,  
 transducers, tires and belts are supposed to endure

R1  
R2  
R3  
R4  
R5  
R6  
R7  
R8  
R9  
R10  
R11  
R12  
R13  
R14  
R15

\*Corresponding author, e-mail: [harea@utb.cz](mailto:harea@utb.cz)  
 © BME-PT

L1 millions of deformation cycles, which can lead to internal  
 L2 micro-failure [13], variation of distances between  
 L3 conductive particles, spatial rearrangements,  
 L4 rotations, possible damage of fillers [6] and changes  
 L5 in the electrical performance of products. That fatigue  
 L6 imposed reorganization of microscopic and meso-  
 L7 scopic structure of carbon black filler in natural rubber  
 L8 was shown in [14]. Presented TEM images demonstrated  
 L9 the destruction of the CB agglomerates and the rearrangement  
 L10 of CB aggregates in a string.  
 L11 The changes in the electrical conductivity of elastomer  
 L12 devices based on CNTs and CB incorporated hybrid filler  
 L13 systems after their extensive fatigue are weakly studied  
 L14 until now. Majority of existing studies on this topic  
 L15 were dedicated to in-situ measurements of conductivity/  
 L16 resistivity during deformation [for example 2, 5, 6] at  
 L17 relatively low frequencies and number of cycles.  
 L18  
 L19 The present work was focused on the preparation of NR  
 L20 composites with hybrid CNTs and CB fillers through a  
 L21 simple mixing method [10] and investigation of their  
 L22 volume conductivity before and after  $10^5$  harmonic  
 L23 sinusoidal loading cycles which was supposed to simulate  
 L24 the long term use of such products as mechano-electrical  
 L25 devices. Implemented number of cycles and low deformation  
 L26 amplitudes, discussed in details in the experimental  
 L27 section of the article, were selected in such a way that  
 L28 they fell far below the mechanical fatigue limit [15] of  
 L29 the rubber matrix. Therefore, all fatigue transformations  
 L30 of the material were supposed to be attributed exclusively  
 L31 to filler network changes. Unusually for electrical  
 L32 properties investigations – 5 Hz frequency of deformation  
 L33 was applied. In each sample, the total amount of fillers  
 L34 was kept at 30 phr level in accordance with simulations  
 L35 [16] which is considered to be the beginning of percolation  
 L36 threshold for CB fillers in elastomers.  
 L37  
 L38

## R1 2. Experimental

### R2 2.1. Materials

R3 Natural rubber used in this research was supplied by  
 R4 the Astlett Rubber Inc. (type SMR 20 CV/BP1). Sulphur  
 R5 used as the curing agent, zinc oxide (ZnO) and stearic  
 R6 acid used as activator and co-activator respectively  
 R7 were supplied by Sigma-Aldrich<sup>®</sup>. Industrial grade  
 R8 of carbon black of the type N220 (Cabot Corporation)  
 R9 was used as filler. CBS (N-cyclohexyl-2-benzothiazole-  
 R10 sulfenamide) was employed as curing accelerator.  
 R11 Toluene used as the swelling solvent in swelling test  
 R12 was supplied by the AnalaR NORMA-PUR<sup>®</sup> ACS. The  
 R13 compounding formulations of the prepared samples along  
 R14 with their short notations are listed in Table 1.

R15 Commonly, CNTs are divided into two categories:  
 R16 single-walled carbon nanotubes (SWCNTs) which  
 R17 consist of a single graphene cylinders, and multi-  
 R18 walled carbon nanotubes (MWCNTs) containing several  
 R19 concentric graphene cylinders. In the present paper  
 R20 MWCNTs were used and are denoted simply as CNTs.  
 R21

R22 Multi-walled carbon nanotubes with diameter of 10–  
 R23 20 nm, bulk density 0.02–0.04 g/cm<sup>3</sup> and surface  
 R24 area in the range of 200–400 m<sup>2</sup>/g, obtained by catalytic  
 R25 pyrolysis described in [17] were provided by  
 R26

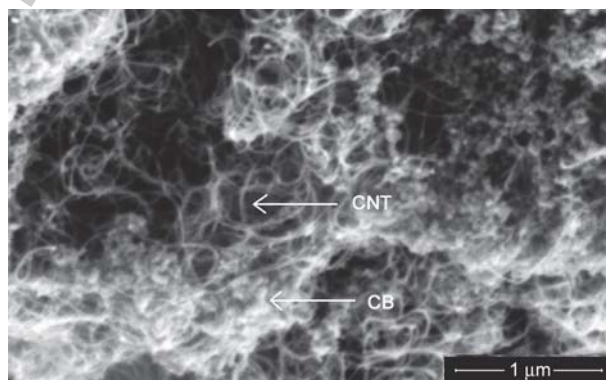


Figure 1. SEM picture of dry mixed CNTs with CB, prepared for sample NR3. Arrows show CNT and CB particles.

Table 1. Samples denotation and composition.

Compounding formulations		NR	CNT+CB	CBS	Sulphur	ZnO	Stearic Acid
		Content [phr] <sup>*</sup>					
Short notations	NR0	100	0+30	1.0	2.5	5.0	2.0
	NR1	100	1+29	1.0	2.5	5.0	2.0
	NR3	100	3+27	1.0	2.5	5.0	2.0
	NR5	100	5+25	1.0	2.5	5.0	2.0

<sup>\*</sup>[phr] – The compound ingredients are given as parts per 100 parts of rubber by weight.

L1 Chuiko Institute of Surface Chemistry, National  
L2 Academy of Sciences of Ukraine. A dry physical  
L3 mixture of carbon black and CNTs filler is shown in  
L4 Figure 1.

## L5 2.2. Rubber compounding

L6 The rubber compounds based on NR filled with CB  
L7 and hybrid CB+CNTs fillers were mixed in a Bra-  
L8 bender Plastograph (Brabender GmbH & Co, Ger-  
L9 many). For each sample, compounding was per-  
L10 formed at 60 °C, at rotor speed of 50 rpm and at a fill  
L11 factor of 80% in weight proportions listed in Table 1.  
L12 After 24 h conditioning at an ambient temperature  
L13 of 20 °C and a relative humidity of 40%, the blends  
L14 were molded into 125×125×2 mm<sup>3</sup> sheets and cured  
L15 in an electrically heated hydraulic press LabEcon  
L16 300 (Fontijne Presses, Netherlands) at 160 °C under  
L17 200 kN force in accordance with the optimum curing  
L18 time established using a moving die rheometer.

## L19 2.3. Testing

L20 Cure characteristics of the compounded samples  
L21 were studied using a Moving Die Rheometer (MDR  
L22 3000 MonTec, Germany) according to ISO 3417 at  
L23 160 °C.

L24 Each molded sheet of about 2 mm in thickness was  
L25 cut into rectangular strips of 45×15 mm<sup>2</sup> (length ×  
L26 width).

L27 DC conductivity was calculated using Equation (1)  
L28 from the current passed through the sample measured  
L29 with a programmable electrometer (Keithley 6517 A,  
L30 USA), at voltage of 3 V during 300 s in geometrical  
L31 center of the strip in a two-point setup, using brass  
L32 plate electrodes of 15 mm diameter (Figure 2) as:

$$L33 \quad \sigma = \frac{I}{U} \cdot \frac{t}{S} \quad (1)$$

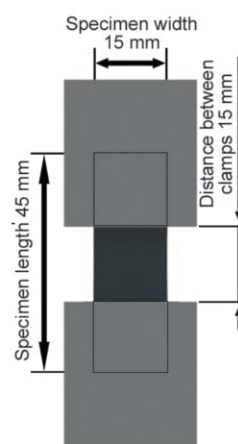
L34 where  $I$  is current,  $U$  is voltage,  $t$  is sample thick-  
L35 ness [cm] and  $S$  is the area of each of the equivalent  
L36 electrodes [cm<sup>2</sup>]. It should be noted that all fatigued  
samples were conditioned for 60±5 min before

measurements in order to minimize elastic recover-  
ing effects.

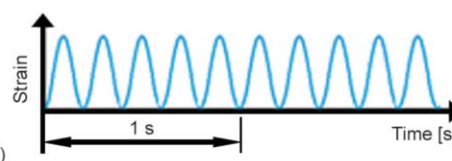
Fatigue measurements were carried out using Tear  
and Fatigue Analyzer (Coesfeld GmbH, Germany).  
The detailed description of the analyzer can be found  
in [18, 19]. Sets of 3 samples per compound at each  
deformation amplitude were analyzed using a fre-  
quency of 5 Hz, the test was carried out up to 10<sup>5</sup> cy-  
cles. Strain amplitudes were set to be 0.1, 0.25 and  
0.50 and initial distance between the clamps was  
15 mm (Figure 3a). The fatigue load was applied  
using sinusoidal waveform (Figure 3b), where the  
pre-stress was set to be 0 MPa.

Images of the hybrid fillers and surface of the pro-  
duced samples were obtained by means of a scanning  
electron microscope (SEM), model Nova NanoSEM  
450 (FEI, USA) with Schottky field emission elec-  
tron source.

Measurement of crosslink density was done through  
the equilibrium solvent swelling method in toluene  
[20]. The samples for test were cut into rectangular



a)



b)

**Figure 3.** a) Clamping system and specimen dimensions, b) harmonic sinusoidal loading procedure.

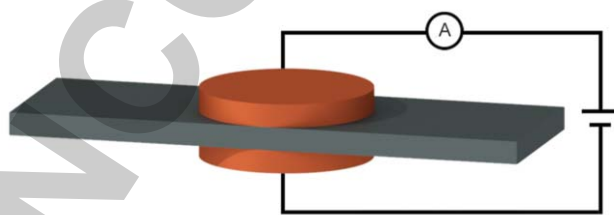
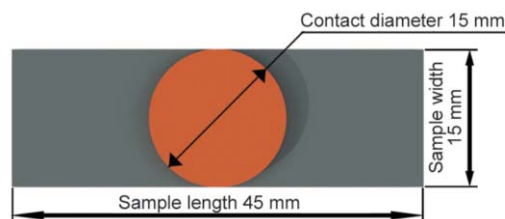


**Figure 2.** Scheme of testing setup.



L1 parallelepipeds measuring  $15 \times 15 \times 2 \text{ mm}^3$  and included  
 L2 the deformed regions of samples after fatigue test  
 L3 and non-deformed regions of as-obtained sheets of  
 L4 rubber composites as well. The test pieces were immersed  
 L5 in toluene at ambient temperature of  $21^\circ\text{C}$ .  
 L6 After 72 h, each sample was withdrawn and the excess  
 L7 of solvent remaining on the surfaces was wiped off  
 L8 with a tissue paper and immediately weighed on an  
 L9 analytical balance. Finally, the sample was dried  
 L10 in a vacuum oven for 12 h at  $50^\circ\text{C}$  and weighed  
 L11 again. The cross-link density  $\nu$  [ $\text{mol}/\text{cm}^3$ ] was calculated  
 L12 by using the Flory–Rehner equation (Equation (2)) [20]:  
 L13

$$\text{L14 } \nu = \frac{-(\ln(1 - \nu_r) + \nu_r + \chi \cdot \nu_r^2)}{V \cdot (\nu_r^{1/3} - \frac{\nu_r}{2})} \quad (2)$$

L15 where  $\chi$  represents the Flory–Huggins interaction parameter  
 L16 between toluene and rubber (0.39),  $V$  is the molar volume  
 L17 of toluene ( $106.3 \text{ cm}^3/\text{mol}$ ). Volume fraction of rubber  
 L18 ( $\nu_r$ ) in the swollen network was calculated by Equation (3):  
 L19

$$\text{L20 } \nu_r = \frac{\frac{W_d - W_f}{\rho_r}}{\frac{W_d - W_f}{\rho_r} + \frac{W_s - W_d}{\rho_s}} \quad (3)$$

L21 where  $W_d$  is the weight of dried sample,  $W_f$  is the  
 L22 weight of the fillers in the sample and  $W_s$  is the weight  
 L23 of the swollen sample.  $\rho_r$  and  $\rho_s$  are the density of  
 L24 rubber ( $0.911 \text{ g}/\text{cm}^3$ ) and the density of solvent  
 L25 ( $0.867 \text{ g}/\text{cm}^3$ ) respectively.

## L26 3. Results and discussion

### L27 3.1. Fatigue dynamic loading

L28 Figure 4 denotes the stress magnitude required to  
 L29 achieve 0.10, 0.25 and 0.50 defined strain for each  
 L30 group of samples consisting of NR0, NR1, NR3 and  
 L31 NR5. All the investigated samples were subjected to  
 L32  $10^5$  fatigue cycles. The data was collected after each  
 L33 100 cycles starting after first 5 cycles, considered as  
 L34 a pre-strain conditioning.

L35 It can be certainly observed that lower strain amplitude  
 L36 required lower stress for all the samples. CNTs  
 L37 loading increased the stress necessary to reach the  
 L38 fixed strain amplitude. As can be seen, the stabilization  
 L39 of stress-strain relations depended on strain amplitude  
 L40 and the composition of fillers. For 0.10 strain  
 L41 amplitude, stabilization was observed from the beginning  
 L42 (just after preconditioning of 5 cycles) for all the  
 L43 studied compositions. Contrary to this, at 0.50 strain

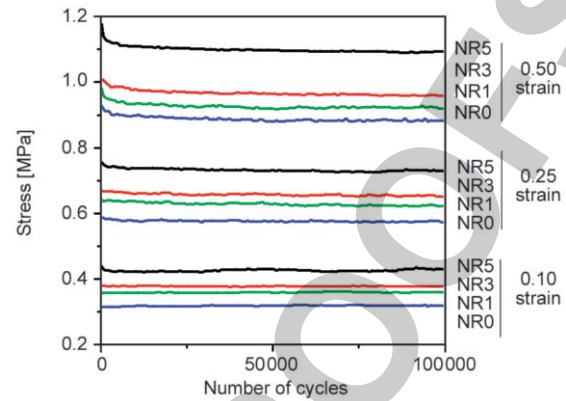


Figure 4. Stress applied to deform samples up to set strain amplitudes (0.10, 0.25 and 0.50) vs. number of fatigue cycles.

testing amplitude, rubber softening lasted up to an  
 unusually high number of 6000 cycles exhibiting the  
 Mullins effect [21]. Whereas, at 0.25 strain amplitude  
 the results were intermediate between the two  
 extremes of 0.10 and 0.50 strains.

### 3.2. Electrical conductivity before fatigue test

Figure 5 shows the DC volume electrical conductivity  
 (calculated using Equation (1)) of the cured samples  
 filled with different ratios of CNT+CB hybrid fillers,  
 before the fatigue tests.

Gradual replacement of pre-defined amount of CB  
 with the same quantity (by weight) of CNTs, namely  
 0.0, 1.0, 3.0, and 5.0 phr, led to very essential growth  
 of conductivity, best represented by the logarithmic  
 scale in Figure 5. Current flow through filled polymers  
 is mainly governed by percolation threshold of matrix-  
 filler system and tunneling effect between conductive  
 fillers [22]. Since, the density of CB ( $\sim 2.2 \text{ g}/\text{cm}^3$ )  
 is close to those of CNT, volume fraction of hybrid  
 fillers can be considered more or less similar for all  
 tested samples.

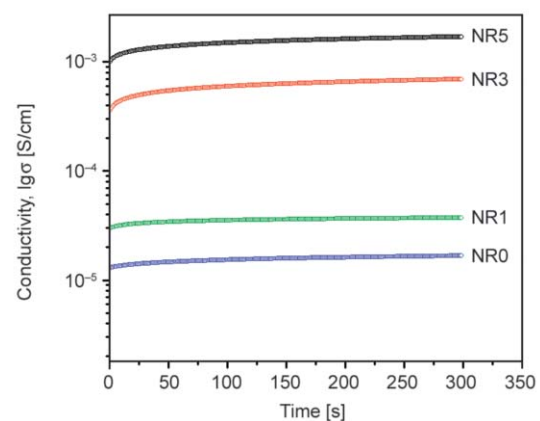


Figure 5. Electrical conductivity of samples before fatigue test.

L1 A pure CB N220 having the average primary particle  
 L2 diameter of about 21 nm and surface area 118 m<sup>2</sup>/g,  
 L3 exhibits moderate electrical conductivity,  $\sigma \sim 2$  S/cm.  
 L4 However, the NR containing 30 phr of CB N220  
 L5 (samples NR0) showed a conductivity of only  
 L6  $\sim 10^{-5}$  S/cm, as is quite expected due to the high vol-  
 L7 ume resistivity of NR.

L8 Addition of CNTs with conductivity  $\sim 10^3$  S/cm, as  
 L9 a part of hybrid fillers, gradually increased the elec-  
 L10 trical conductivity of NR/CB+CNTs composite up  
 L11 to  $\sim 10^{-3}$  S/cm (for samples NR5). The other samples  
 L12 showed somewhat lesser magnitudes, though exhibit-  
 L13 ing an increasing trend with increase in concentra-  
 L14 tion of CNTs.

L15 Figure 5 also reflects an increase in conductivity as  
 L16 a function of time. The conductivity of the samples  
 L17 increased with time, initially very rapidly, then more  
 L18 slowly, approaching a quasi-equilibrium value. Ac-  
 L19 cording to [23], the carbon black particles are con-  
 L20 nected to each other by the flexible long rubber mole-  
 L21 cules. The flexibility of the rubber molecules allows  
 L22 almost free translational kinetic (Brownian) motion  
 L23 of the carbon black particles, up to the limit given  
 L24 by the length of the rubber molecules and enhances  
 L25 filled polymer conductivity in time.  
 L26 This phenomenon never stops but after sufficient  
 L27 time, a quasi-equilibrium of conductivity is estab-  
 L28 lished.

### L29 3.3. Electrical conductivity after fatigue test

L30 The conductivity measured after fatigue test was also  
 L31 a time dependent process and presented results (Fig-  
 L32 ure 6) are the arithmetic mean values of each set of  
 L33 samples in the steady-state conductivity regime. For  
 L34 better understanding of the exact magnitudes, the nu-  
 L35 merical values are presented in Table 2.

L36 The highest modification in conductivity after fa-  
 L37 tigue test was observed in case of NR0 where CNTs  
 L38 were absent and the higher fatigue strain amplitude  
 L39 produced higher conductivity degeneration. This  
 L40 trend was generally found for all the compositions

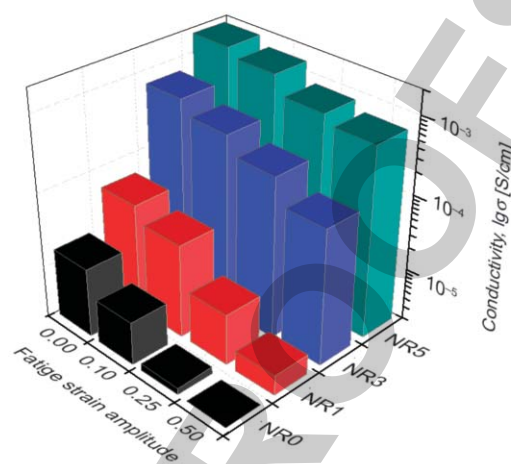


**Figure 6.** Conductivity of composites before (0.0 strain amplitude) and after fatigue test at 0.10, 0.25 and 0.50 strain amplitude vs. CNTs concentration in composites: NR0 – 0.0 phr, NR1 – 1.0 phr, NR3 – 3.0 phr and NR5 – 5.0 phr of CNTs content.

of the samples. However, increased quantity of CNTs in hybrid fillers preserved the electrical properties of nanocomposites subjected to fatigue processes, in a much better way. For example, after fatigue test at 0.50 strain amplitude samples containing 5 phr of CNTs showed 2.7 times decreased conductivity against 33.3 times decreased conductivity for samples without CNTs.

Generally, for cyclic deformation of vulcanizates at high strains, the material microstructure evolution can be divided into two stages. First is the network decomposition process into a pure rubber network phase and a polymer-filler network phase [24]. The second stage induces more dramatic changes and is characterized by cavitation induced by decohesion between hard particles and soft rubber matrix (for example between zinc oxide and NR [25]).

In the present work, cyclic stretching tests of samples were carried out at low strain amplitudes which were below the mechanical fatigue limit [15] of rubber matrix. Thus, it was assumed that only the filler network was mainly modified leaving the rubber matrix almost intact. SEM analyses of surface morphology

**Table 2.** Electrical conductivity of samples before and after  $10^5$  cycles of deformation at 0.10, 0.25 and 0.50 of strain amplitude.

	NR0 conductivity [S/cm]	NR1 conductivity [S/cm]	NR3 conductivity [S/cm]	NR5 conductivity [S/cm]
Before fatigue test	$1.7 \cdot 10^{-5}$	$5.8 \cdot 10^{-5}$	$7.3 \cdot 10^{-4}$	$1.9 \cdot 10^{-3}$
0.10 strain, $10^5$ cycles	$7.6 \cdot 10^{-6}$	$3.6 \cdot 10^{-5}$	$4.8 \cdot 10^{-4}$	$1.5 \cdot 10^{-3}$
0.25 strain, $10^5$ cycles	$2.5 \cdot 10^{-6}$	$9.5 \cdot 10^{-6}$	$2.8 \cdot 10^{-4}$	$8.8 \cdot 10^{-4}$
0.50 strain, $10^5$ cycles	$5.1 \cdot 10^{-7}$	$3.7 \cdot 10^{-6}$	$1.3 \cdot 10^{-4}$	$6.9 \cdot 10^{-4}$

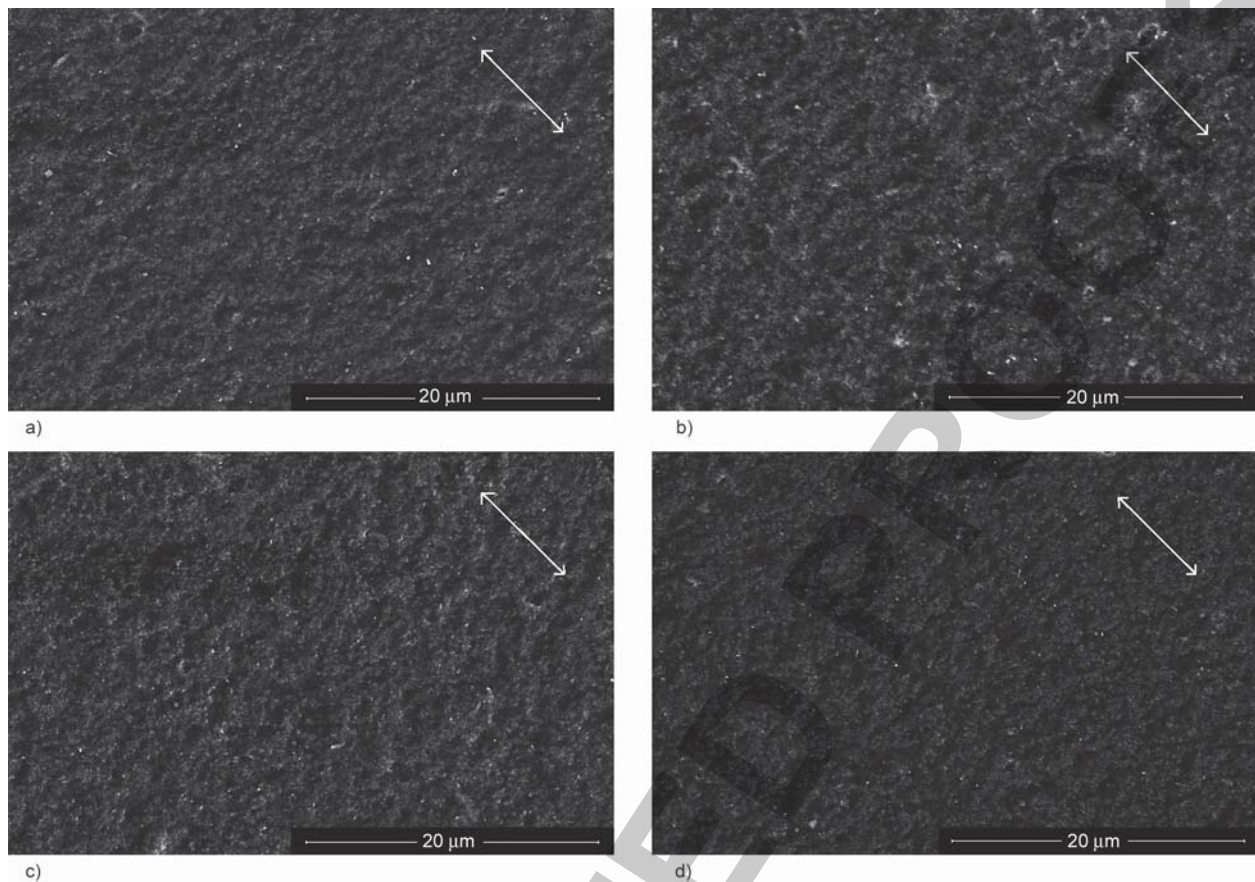


**Figure 7.** SEM images of in-situ 0.5 strained samples of NR5 composition: a) as obtained, b) after fatigue test at 0.10 test amplitude, c) after fatigue test at 0.25 test amplitude and d) after fatigue test at 0.50 test amplitude. White arrows show the direction of in-situ elongation as well the direction of fatigue test.

L1 of the unfatigued as well as the fatigued samples at  
 L2 all the three test amplitudes revealed lack of cracks  
 L3 in polymer visible at micro level, as is shown in Fig-  
 L4 ure 7. In order to open the cracks and make them ob-  
 L5 servable, the samples were strained at 0.5 during the  
 L6 SEM analyses. The examined morphology of the rub-  
 L7 ber polymer reflected non-appearance of any cracks  
 L8 at selected magnification as well as no remarkable  
 L9 differences between samples.

L10 Another more sensitive method (besides SEM), to  
 L11 perceive any breaks of rubber matrix even at molecu-  
 L12 lar level is swelling test. Figure 8 summarizes the  
 L13 crosslink density (obtained from Equation (2)) of  
 L14 vulcanizates with different CB+CNTs contents be-  
 L15 fore and after fatigue test at different strain ampli-  
 L16 tudes. The crosslink density of vulcanizates exhib-  
 L17 ited an increasing trend with an increase in CNTs con-  
 L18 tent. This was attributed to the physical crosslinks  
 L19 between CNTs and natural rubber [20], which im-  
 L20 mobilized the rubber chains and consequently min-  
 L21 imized the amount of the solvent within the rubber  
 L22 matrix at equilibrium swelling. All fatigue tested  
 L23 samples, subjected to different strain amplitudes,

showed slight reduction in crosslink density com-  
 pared to the non-fatigued ones and no significant  
 change with an increase in strain amplitude. This ex-  
 perimentally confirmed that no critical transforma-  
 tion occurred in the rubber matrix during cyclic uni-  
 axial tensile test at the implemented strain ampli-  
 tudes and number of cycles. On the other hand, elec-  
 trical conductivity degradation strongly indicated a  
 residual restructuring of conductive paths. Therefore,

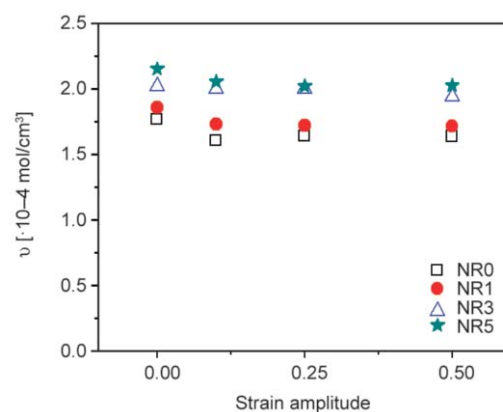


**Figure 8.** Crosslink density of vulcanizates before and after fatigue test at different strain amplitudes.

L1 fatigue transformation in investigated vulcanizates  
 L2 at small strain amplitudes (up to 0.5) was predomi-  
 L3 nantly due to reorganization of CB filler network  
 L4 (filler network breakdown, filler deagglomeration in  
 L5 the framework of self-similarity, polymer debonding  
 L6 from filler surface, strain softening of the polymer  
 L7 shell surrounding fillers, a network junction at small  
 L8 strain, or the jamming transition [26] etc.).

L9 All these processes might have led to significant de-  
 L10 struction of the conductive paths which was hypoth-  
 L11 esized through an indigenous scheme shown in Fig-  
 L12 ure 9. In the figure white lines show the conductive  
 L13 paths which cross the presented region in vertical di-  
 L14 rection. The blue structures signify nanotubes while  
 L15 red dots are carbon black particles.

L16 The carbon black primary particles almost never  
 L17 exist separately and are strongly fused by covalent  
 L18 bonds into aggregates which join together by van der  
 L19 Waals forces and form agglomerates.

L20 During the external stressed condition, the strain of  
 L21 rubber matrix at the nano level, is assumed to be very  
 L22 non-uniform and filler dependent. The investigated  
 L23 samples could be regarded as a mixture of domains  
 L24 with different elastic modulus and rupture strength  
 L25 (depending on local concentration of fillers). The re-  
 L26 gions with low concentration of fillers are more  
 L27 stretchable. Due to this strain gradient, it can be as-  
 L28 sumed that the slipping of molecular rubber chains  
 L29 over surfaces of CB aggregates [27], will be oriented  
 L30 toward the regions with lower concentration of fillers.  
 L31 Thus enlarging of nonconductive regions is accom-  
 L32 panied by separation of peripheral aggregates from  
 L33 agglomerates, simultaneous compaction of aggre-  
 L34 gates which form the core of agglomerates and broad  
 L35 destruction of conductive paths. Due to their high as-  
 L36 pect ratio, and surrounding rubber chain immobility  
 L37 [20], CNTs may arrest the increasing or formation

of nonconductive regions in its vicinity. Thus, the  
 electro-conductive paths containing only CB are  
 much more affected in the process of destruction  
 than the paths containing CB+CNTs. More than that,  
 a fatigued sample is supposed to concentrate the CB  
 agglomerates around of relatively fixed CNTs and  
 generate CNTs dependent distribution of reformed  
 conductive spots (Figure 9b). These reformations of  
 conductive paths, ultimately led to decreasing of con-  
 ductivity compared to initial samples but higher con-  
 centration of CNTs much better preserve the conduc-  
 tivity in fatigued samples.

#### 4. Conclusions

Long lasting cyclic deformation at strain amplitudes  
 up to 0.5 did not exhibit change in NR polymer ma-  
 trix filled with hybrid filler but substantially changed  
 the residual electrical conductivity of tested samples.  
 With an increase in cyclic deformation amplitude,  
 the residual electrical conductivity of all the samples  
 decreased.

Partial replacement of CB with CNTs definitely im-  
 proved volume conductivity of the unstrained sam-  
 ples. Also, increasing amount of CNTs in the hybrid  
 systems tended to better preserve the conductivity  
 after cyclic deformation due to its active role in re-  
 stricting the formation of nonconductive regions be-  
 tween CB agglomerates. This tendency may be very  
 much appreciated in fabrication of transducers, sen-  
 sors and flexible electrodes working under elastical-  
 ly deformed conditions as well as in applications for  
 electrostatic rubber products.

Related to the results of the experiments, a new  
 mechanism of ‘conductivity preservation’ in flexible  
 conductive materials based on CB+CNTs hybrid  
 fillers was proposed, and explained through the re-  
 organization of the positions of CB aggregates  
 against CNTs.

#### Acknowledgements

This article was written with the support of Operational Pro-  
 gram Research and Development for Innovations co-funded  
 by the European Regional Development Fund and national  
 budget of the Czech Republic, within the framework of the  
 project CPS—strengthening research capacity [reg. number:  
 CZ.1.05/2.1.00/19.0409] as well supported by the Ministry  
 of Education, Youth and Sports of the Czech Republic – Pro-  
 gram NPU I [LO1504] and by the internal grant agency of  
 the project IGA/CPS/2019/001.

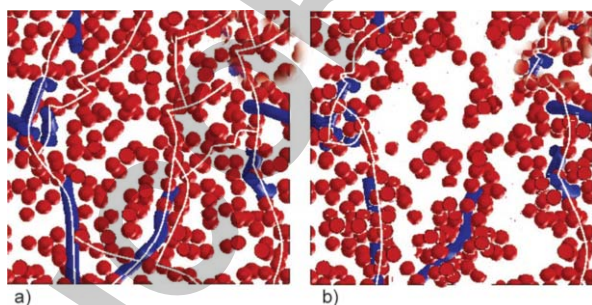


**Figure 9.** Scheme of conductive paths inside of sample containing hybrid filler: a) before and b) after fatigue test.

L1 **References**

- L2 [1] Boonstra B. B. S. T., Dannenberg E. M.: Electrical con-  
L3 ductivity of rubber-carbon black vulcanizates. *Industrial*  
L4 *and Engineering Chemistry*, **46**, 218–227 (1954).  
L5 <https://doi.org/10.1021/ie50529a064>
- L6 [2] Natarajan T. S., Eshwaran S. B., Stöckelhuber K. W.,  
L7 Wießner S., Pötschke P., Heinrich G., Das A.: Strong  
L8 strain sensing performance of natural rubber nanocom-  
L9 posites. *ACS Applied Materials and Interfaces*, **9**, 4860–  
L10 4872 (2017).  
L11 <https://doi.org/10.1021/acsami.6b13074>
- L12 [3] Ishigure Y., Iijima S., Ito H., Ota T., Unuma H., Taka-  
L13 hashi M., Hikichi Y., Suzuki H.: Electrical and elastic  
L14 properties of conductor-polymer composites. *Journal of*  
L15 *Materials Science*, **34**, 2979–2985 (1999).  
L16 <https://doi.org/10.1023/A:1004664225015>
- L17 [4] Liu P., Liu C., Huang Y., Wang W., Fang D., Zhang Y.,  
L18 Ge Y.: Transfer function and working principle of a  
L19 pressure/temperature sensor based on carbon black/sil-  
L20 icon rubber composites. *Journal of Applied Polymer*  
L21 *Science*, **133**, 42979–42988 (2016).  
L22 <https://doi.org/10.1002/app.42979>
- L23 [5] Ciselli P., Lu L., Busfield J. J. C., Peijs T.: Piezoresis-  
L24 tive polymer composites based on EPDM and MWNTs  
L25 for strain sensing applications. *e-Polymers*, **10**, 1–13  
L26 (2010).  
L27 <https://doi.org/10.1515/epoly.2010.10.1.125>
- L28 [6] De Focatiis D. S. A., Hull D., Sanchez-Valencia A.:  
L29 Roles of prestrain and hysteresis on piezoresistance in  
L30 conductive elastomers for strain sensor applications.  
L31 *Plastics, Rubber and Composites*, **41**, 301–309 (2012).  
L32 <https://doi.org/10.1179/1743289812Y.0000000022>
- L33 [7] Salaeh S., Nakason C.: Influence of modified natural  
L34 rubber and structure of carbon black on properties of  
L35 natural rubber compounds. *Polymer Composites*, **33**,  
L36 489–500 (2012).  
L37 <https://doi.org/10.1002/pc.22169>
- L38 [8] Abdul-Salim Z. A. S., Hassan A., Ismail H.: A review  
L39 on hybrid fillers in rubber composites. *Polymer-Plastics*  
L40 *Technology and Engineering*, **57**, 523–539 (2018).  
L41 <https://doi.org/10.1080/03602559.2017.1329432>
- L42 [9] Dong B., Liu C., Lu Y., Wu Y.: Synergistic effects of  
L43 carbon nanotubes and carbon black on the fracture and  
L44 fatigue resistance of natural rubber composites. *Journal*  
L45 *of Applied Polymer Science*, **132**, 42075–42083 (2015).  
L46 <https://doi.org/10.1002/app.42075>
- L47 [10] Harea E., Stoček R., Storozhuk L., Sementsov Y., Kar-  
L48 tel N.: Study of tribological properties of natural rubber  
L49 containing carbon nanotubes and carbon black as hy-  
L50 brid fillers. *Applied Nanoscience*, **9**, 899–906 (2018).  
L51 <https://doi.org/10.1007/s13204-018-0797-6>
- L52 [11] Nakaramontri Y., Pichaiyut S., Wisunthorn S., Nakason  
L53 C.: Hybrid carbon nanotubes and conductive carbon  
L54 black in natural rubber composites to enhance electrical  
L55 conductivity by reducing gaps separating carbon nano-  
L56 tube encapsulates. *European Polymer Journal*, **90**,  
L57 467–484 (2017).  
L58 <https://doi.org/10.1016/j.eurpolymj.2017.03.029>
- [12] Ma P-C., Liu M-Y., Zhang H., Wang S-Q., Wang R.,  
Wang K., Wong Y-K., Tang B-Z., Hong S-H., Paik K-W.,  
Kim J-K.: Enhanced electrical conductivity of nano-  
composites containing hybrid fillers of carbon nano-  
tubes and carbon black. *ACS Applied Materials and*  
*Interfaces*, **1**, 1090–1096 (2009).  
<https://doi.org/10.1021/am9000503>
- [13] Huneau B., Masquelier I., Marco Y., le Saux V., Noizet  
S., Schiel C., Charrier P.: Fatigue crack initiation in a  
carbon black-filled natural rubber. *Rubber Chemistry*  
*and Technology*, **89**, 126–141 (2016).  
<https://doi.org/10.5254/rct.15.84809>
- [14] Sun C., Du Z., Nagarajan S., Zhao H., Wen S., Zhao S.,  
Zhang P., Zhang L.: Impact of uniaxial tensile fatigue  
on the evolution of microscopic and mesoscopic struc-  
ture of carbon black filled natural rubber. *Royal Society*  
*Open Science*, **6**, 181883/1–181883/10 (2019).  
<https://doi.org/10.1098/rsos.181883>
- [15] Lake J., Lindley P. B.: Fatigue of rubber at low strains.  
*Journal of Applied Polymer Science*, **10**, 343–351  
(1966).  
<https://doi.org/10.1002/app.1966.070100214>
- [16] Schwatz G., Cerveny S., Marzocca A.: A numerical  
simulation of the electrical resistivity of carbon black  
filled rubber. *Polymer*, **41**, 6589–6595 (2000).  
[https://doi.org/10.1016/S0032-3861\(99\)00894-0](https://doi.org/10.1016/S0032-3861(99)00894-0)
- [17] Yanchenko V. V., Sementsov Y., Melezhyk A. V.: Process  
for preparation of carbon nanotubes (in Russian). U.A.  
Patent 69292, Ukraine (2007).
- [18] Eisele U., Kelbch S. A., Engels H-W.: The tear analyzer  
– A new tool for quantitative measurements of the dy-  
namic crack growth of elastomers. *Kautschuk und*  
*Gummi Kunststoffe*, **45**, 1064–1069 (1992).
- [19] Stoček R., Heinrich G., Gehde M., Kipscholl R.: Analy-  
sis of dynamic crack propagation in elastomers by si-  
multaneous tensile- and pure-shear-mode testing. in  
‘Fracture mechanics and statistical mechanics of rein-  
forced elastomeric blends’ (eds.: Grellmann W., Heinrich  
G., Kaliske M., Klüppel M., Schneider K., Vilgis T.)  
Springer, Berlin, Vol **70**, 269–301 (2013).  
[https://doi.org/10.1007/978-3-642-37910-9\\_7](https://doi.org/10.1007/978-3-642-37910-9_7)
- [20] Zhan Y. H., Liu G. Q., Xia H. S., Yan N.: Natural rub-  
ber/carbon black/carbon nanotubes composites pre-  
pared through ultrasonic assisted latex mixing process.  
*Plastics, Rubber and Composites*, **40**, 32–39 (2011).  
<https://doi.org/10.1179/174328911X12940139029284>
- [21] Mullins L.: Softening of rubber by deformation. *Rubber*  
*Chemistry and Technology*, **42**, 339–362 (1969).  
<https://doi.org/10.5254/1.3539210>
- [22] Sherman R. D., Middleman L. M., Jacobs S. M.: Elec-  
tron transport processes in conductor-filled polymers.  
*Polymer Engineering and Science*, **23**, 36–46 (1983).  
<https://doi.org/10.1002/pen.760230109>
- [23] Wack P. E., Anthony R. L., Guth E.: Electrical conduc-  
tivity of gr-s and natural rubber stocks loaded with  
Shawinigan and R-40 blacks. *Journal of Applied*  
*Physics*, **18**, 456/1–456/14 (1947).  
<https://doi.org/10.1063/1.1697676>



- L1 [24] Dargazany R., Itskov M.: A network evolution model R1  
L2 for the anisotropic Mullins effect in carbon black filled R2  
L3 rubbers. International Journal of Solids and Structures, R3  
L4 **46**, 2967–2977 (2009).  
L5 <https://doi.org/10.1016/j.ijsolstr.2009.03.022>  
L6 [25] le Cam J-B., Huneau B., Verron E., Gornet L.: Mechanism of fatigue crack growth in carbon black filled natural rubber. Macromolecules, **37**, 5011–5017 (2004).  
L7  
L8  
L9 <https://doi.org/10.1021/ma0495386>
- [26] Hentschke R.: The Payne effect revisited. Express Polymer Letters, **11**, 278–292 (2017).  
<https://doi.org/10.3144/expresspolymlett.2017.28>
- [27] Mostafa A., Abouel-Kasem A., Bayoumi M., El-Sebaie M.: Rubber-filler interactions and its effect in rheological and mechanical properties of filled compounds. Journal of Testing and Evaluation, **38**, 347–359 (2010).  
<https://doi.org/10.1520/JTE101942>
- R4  
R5  
R6  
R7  
R8

**Author Query Form****(EPL\_0010118)**

If you would like to request changes in the proof you are kindly asked to use the commenting tools of your PDF software. If this option is not available for you, please list the necessary corrections in a separate DOC file, indicating the page and the exact line number of the proof.

Hand-written corrections are not accepted.

We would like to draw your attention that you may not request major corrections or inclusions in this final stage of the manuscript. Thank you for your understanding.

Furthermore you are kindly requested to respond the following queries: